JBC Papers in Press. Published on October 11, 2012 as Manuscript M112.407957
The latest version is at http://www.jbc.org/cgi/doi/10.1074/jbc.M112.407957

APOE4-specific changes in Aβ accumulation in a new transgenic mouse model of Alzheimer's disease

Katherine L. Youmans[1a], Leon M Tai[1], Evelyn Nwabuisi-Heath[1], Lisa Jungbauer[1b], Takahisa Kanekiyo[2], Ming Gan[2], Jungsu Kim[3], William A. Eimer[4], Steve Estus[5], G. William Rebeck[6], Edwin J Weeber[7], Guojun Bu[2], Chunjiang Yu[1] and Mary Jo LaDu[1]

From the [1]Department of Anatomy and Cell Biology, University of Illinois at Chicago, Chicago, IL 60612; [2]Department of Neuroscience, Mayo Clinic, Jacksonville, FL 32224; [3]Department of Neurology, Washington University School of Medicine, St. Louis, MO 63110; [4]Department of Cell and Molecular Biology, Feinberg School of Medicine, Northwestern University, Chicago, IL 60611; [5]Sanders-Brown Center on Aging, University of Kentucky, Lexington, KY 40536; [6]Department of Neuroscience, Georgetown University, Washington, DC 20057; [7]Department of Molecular Pharmacology and Physiology, University of South Florida, Tampa, FL 33613.
Present affiliations: [a]Department of Pharmacology, Boston University, Boston, MA 02215
[b]Medtronic Inc., Minneapolis, Minnesota, USA

Running title: APOE4-specific changes in Aβ accumulation in AD Tg-mice

To whom all correspondence should be addressed: Mary Jo LaDu, University of Illinois at Chicago, Department of Anatomy and Cell Biology, 808 S.Wood St., M/C 512, Chicago, IL 60612, USA. Phone: 312-355-4795; Fax: 312-413-0354; Email: mladu@uic.edu

Keywords: APOE genotype; amyloid-β; Alzheimer's disease; soluble Aβ species, AD transgenic mouse model

Background: *APOE*-genotype effects on different forms of Aβ accumulation were determined using new EFAD transgenic mice.
Results: In E4FAD mice, compact/diffuse plaques are greater, total apoE4 is lower, less apoE4 is lipoprotein-associated, and soluble Aβ42 and oligomeric-Aβ are higher than E2FAD/E3FAD. Intraneuronal Aβ is comparable across *APOE*-genotype.
Conclusion: *In vivo*, *APOE4* uniquely effects Aβ accumulation.
Significance: These data suggest a basis for *APOE*-induced AD risk.

ABSTRACT

APOE4 is the greatest risk factor for Alzheimer's disease (AD) and synergistic effects with amyloid-β peptide (Aβ) suggest interactions among apoE isoforms and different forms of Aβ accumulation. However, it remains unclear how *APOE* genotype affects plaque morphology, intraneuronal Aβ, soluble Aβ42, and oligomeric Aβ (oAβ), particularly *in vivo*. As introduction of human *APOE* significantly delays amyloid deposition in transgenic mice expressing familial-AD (FAD) mutations (FAD-Tg), 5xFAD-Tg mice, which exhibit amyloid deposition by 2-months, were crossed with apoE targeted-replacement mice to produce the new EFAD-Tg mice. Compared to 5xFAD mice, Aβ deposition was delayed ~4 months in the EFAD mice, allowing detection of early changes in Aβ accumulation from 2-6 months. While plaque deposition is generally greater in E4FAD mice, E2/E3FAD have significantly more diffuse and E4FAD more compact plaques. As a first report in FAD-Tg mice, *APOE* genotype had no effect on intraneuronal Aβ accumulation in EFAD mice. In E4FAD mice, total apoE levels were lower and total Aβ levels higher than E2FAD and E3FAD mice. Profiles from sequential three-step extractions (TBS, detergent and formic acid) demonstrate that the lower level of total apoE4 is reflected only in the detergent-soluble fraction, indicating that less apoE4 is lipoprotein-associated, and perhaps less lipidated, compared with apoE2 and apoE3. Soluble Aβ42 and oAβ levels were highest in E4FAD mice, although soluble apoE2, apoE3 and apoE4 levels were comparable, suggesting that the differences in soluble Aβ42 and oAβ result from functional

Copyright 2012 by The American Society for Biochemistry and Molecular Biology, Inc.

Downloaded from www.jbc.org at University of Illinois at Chicago Library, on October 29, 2012

differences among the apoE isoforms. Thus, *APOE* differentially regulates multiple aspects of Aβ accumulation.

INTRODUCTION

The primary genetic risk factor for Alzheimer's disease (AD) is *APOE4,* increasing risk ~4- and 15-fold with a single or double allele(s), while *APOE2* reduces risk compared to *APOE3.* Although carriers of the *APOE4* gene of apolipoprotein E (apoE) account for more than half of AD patients, the mechanism(s) by which *APOE* affects the pathogenesis of AD is the subject of continued inquiry (1). Plaque deposition is increased with *APOE4* compared with *APOE2* and *APOE3* in humans and transgenic mice expressing familial-AD (FAD) mutations (FAD-Tg) (2-5). However, an *APOE* genotype-specific effect on the accumulation of other potentially neurotoxic species of Aβ remains unclear. Research efforts to address this mechanism *in vivo* are hindered by the lack of: 1) tractable transgenic mouse models and; 2) assays for changes in Aβ speciation and apoE solubility during the initial stages of Aβ accumulation.

Introduction of human *APOE* to existing FAD-Tg mice significantly delays plaque deposition, although once detected, plaque levels are generally greater with *APOE4* than *APOE3* (3,6-8). For example, crossing apoE-targeted-replacement mice (apoE-TR) (9) with PDAPP mice (10) delays plaque deposition from ~10 to 18 months; although once detected, plaque levels are greater with *APOE4* than *APOE3* (3). To establish a tractable model, transgenic mice expressing 5 FAD mutations (5xFAD), which exhibit accelerated plaque deposition that is significant by 2 months (11), were crossed with apoE-TR mice to produce the EFAD mouse model. In EFAD mice, *APOE* genotype-specific effects on Aβ accumulation can be identified from 2 to 6 months.

Aβ pathology can refer to a number of neurotoxic forms of the peptide, making identification of "neurotoxic Aβ" unclear. Detection of different Aβ species requires complimentary immunohistochemical (IHC) and biochemical approaches. By IHC, intraneuronal Aβ (12-14), and perhaps specific plaque morphologies (15,16) are thought to contribute to Aβ pathology, although amyloid plaque burden *per se* may not be neurotoxic (17). Biochemical analysis has demonstrated that oAβ (18-21) and soluble Aβ levels are elevated in AD brains (18) and soluble oligomeric forms of Aβ42 have been demonstrated to correlate with cognitive decline (20) and disease severity in humans (22). *APOE* genotype may affect AD risk by modulating the speciation of Aβ42, particularly oAβ levels. Possible mechanisms for this apoE isoform-specific effect include differences in Aβ clearance, degradation and/or stabilization of oAβ (for review (23)). Specific detection methods for oAβ are one factor limiting further understanding of apoE isoform-specific effects on oAβ levels. Thus, an ELISA for measuring oAβ levels was developed following the protocol of Xia and co-workers (24), enabled by the development of the new Aβ-specific antibody MOAB-2 (25).

Total apoE4 levels are lower compared with apoE2 and apoE3 in human plasma and CSF for both AD patients (26-31) and age-matched controls (32), brain homogenates from AD patients (3,33), brain homogenates from apoE-TR mice (3,28,34), and brain homogenates from apoE-TR/PDAPP-Tg mice (3). However, it is not known whether biochemical methods for sequential extraction differentially affect apoE isoform levels (3,35). Traditionally, a non-ionic detergent is required to release apoE from lipoprotein particles (i.e. Triton X-100; TBSX) without inducing the formation of new micelles, as can occur with ionic detergents such as SDS (36) (35,37-41). To address this issue, a 3-step, sequential protein extraction protocol was optimized to account for the extraction conditions for lipoprotein-associated apoE, as well as insoluble protein from dense-core amyloid plaques (42).

In this study, development of the EFAD transgenic mouse model enabled identification of the effects of *APOE* genotype on early types of Aβ accumulation. From 2 to 6 months, plaque deposition was generally greater in E4FAD mice, although E2FAD and E3FAD had primarily diffuse and E4FAD compact plaques, while intraneuronal Aβ levels were comparable among the *APOE* genotypes. Biochemical measurements of total apoE and Aβ levels, combined with an

Downloaded from www.jbc.org at University of Illinois at Chicago Library, on October 29, 2012

extraction method to isolate and identify the soluble, detergent and insoluble levels of apoE, Aβ, and oAβ, revealed mechanistic interplay between the apoE isoforms and these defined species of Aβ. While total apoE4 levels were lower than apoE2 and apoE3, as previously demonstrated, of particular importance is the novel finding that the decreased levels of total apoE4 occur only in the TBSX extraction fraction, demonstrating that less apoE4 is lipoprotein-associated, and perhaps apoE4 is less lipidated, compared with apoE2 and apoE3. In addition, the levels of soluble Aβ42 and oAβ are higher with apoE4.

EXPERIMENTAL PROCEDURES

EFAD mice development

Experiments follow the UIC Institutional Animal Care and Use Committee protocols. All breeding and colony maintenance was conducted at Taconic labs. 5xFAD mice co-express 5 FAD mutations (APP K670N/M671L + I716V + V717I and PS1 M146L + L286V) under the control of the neuron-specific mouse Thy-1 promoter (11). The 5xFAD line Tg6799 that produce the highest amount of Aβ and are heterozygous for the 5xFAD genes was provided by Dr. R. Vassar (Northwestern University). In apoE-TR mice, the coding region of the human *APOE* gene replaces that of the mouse *APOE* gene. Homozygous apoE-TR mice were purchased from Taconic in collaboration with Dr. P. Sullivan (Duke University)(9,43). Details on the production, genotyping, and genetic background of these mice are described in the above papers.

To establish colonies of EFAD mouse lines (E2FAD, E3FAD and E4FAD), 5xFAD mice were bred to homozygous APOE2-, APOE3- and APOE4-TR mice by Taconic labs. Briefly, male APOE-TR$^{+/+}$ mice on a C57/B6 background were bred with female 5xFAD$^{+/-}$ mice on a C57B//B6xSJL background. The resulting female mouse-APOE/APOE-TR/5xFAD$^{+/-}$ mice were backcrossed with male APOE-TR mice to generate APOE-TR$^{+/+}$/5xFAD$^{+/-}$ (EFAD) mice. In this study male EFAD mice were utilized. Female mice were excluded from this initial study for consistency, as apoE isoform-specific interaction with Aβ are known to be influenced by gender (for review (44)). In EFAD mice, the levels of full-length APP were equivalent among the *APOE* genotypes (Supplementary Figure 1). This suggests that any observed *APOE* genotype-specific differences in Aβ accumulation are not mediated by altered APP expression or processing. These results are consistent with results from the PDAPP/apoE-TR mice (3) and J20/APOEfKI (45) where no significant differences in APP levels were observed with *APOE* genotype.

Tissue Harvesting

2, 4 and 6 month old mice were anesthetized with sodium pentobarbital (50mg/kg) and transcardially perfused with ice-cold PBS containing protease inhibitors (Calbiochem, set 3). Directly following perfusion, brains were removed and dissected at the midline. Left hemi-brains from mice at each age were drop-fixed in 4% paraformaldehyde (PFA) for 48 h followed by storage at 4°C in PBS + 0.05% sodium azide (NaN_3) until use. Right hemi-brains were dissected on ice into cortex (CX), hippocampus (H) and cerebellum (CB), immediately snap frozen in liquid nitrogen, and stored at -80°C until use.

Immunohistochemistry for Aβ

PFA-fixed left hemi-brains were incubated in two sequential 30% sucrose solutions (in TBS) for 24 h each, frozen on dry ice, cut sagittally at 35μm thickness on a sliding microtome and sections were stored in cryoprotectant at -20°C. Immediately prior to staining, tissue sections were washed in TBS (3 x 10 min), incubated in 88% formic acid (FA) (8 min), permeabilized with 0.25% Triton X-100 in TBS (TBST; 3 x 10 min) and blocked with 5% bovine serum albumin (BSA) in TBST for 1hr. Free-floating sections were subsequently incubated with an anti-Aβ antibody MOAB-2 (mouse IgG_{2b}, 1:1000 dilution of 0.5mg/ml stock (25)) and an anti-NeuN antibody (mouse IgG_1, 1:1000 dilution, Chemicon) diluted in TBST, containing 2% BSA overnight on an oscillatory rotator. Next, sections were washed in TBST (6 x 10 min), incubated with Alexa fluorophore-conjugated isotype specific secondary antibodies diluted 1:200 in TBST containing 2% BSA for 1 h, washed in TBST (3 x 10 min), washed in TBS (3 x 10 min), and mounted on glass coverslips with ProLong

Downloaded from www.jbc.org at University of Illinois at Chicago Library, on October 29, 2012

Gold antifade mounting media containing DAPI (Invitrogen). Images were captured on a Zeiss Axio Imager M1 under identical capture settings, at 20x or 63x magnification.

Protein Extractions

Serial extractions of brain tissue were performed essentially as described (42). Briefly, frozen tissue from dissected brains was homogenized in 15 volumes (w/v) of TBS. Samples were centrifuged (100,000xg, 1 h at 4°C) and the TBS-soluble fraction was aliquoted prior to freezing in liquid nitrogen and storage at -80°C. The pellet was washed in TBS, resuspended in 15 volumes of TBS buffer containing 1% Triton X-100 (TBSX) and mixed gently by rotation at 4°C for 30 min. Samples were centrifuged (100,000xg, 1 h at 4°C) and the TBSX-soluble fraction was aliquoted and frozen as for TBS. The pellet was washed with TBSX, resuspended in 70% FA to 150mg/ml based on pellet weight and mixed by rotation at room temperature for 2 h with occasional vortexing. Samples were centrifuged (100,000xg 1 h at 4°C), the FA-soluble fraction neutralized (with 20 volumes 1M Tris base), aliquoted and frozen at -80°C. Total protein content in TBS- and TBSX-extractions was determined via colorimetric micro-BCA assay per manufacturer's instructions (Thermo-Scientific). Due to interference of Tris and FA with the BCA assay, total protein in FA-extractions was determined via Quick Start Bradford Protein micro-Assay.

ELISAs

ApoE and Aβ42: ApoE levels were determined as previously described (42), using apoE2, E3 and E4 standards (Calbiochem) (0-100 ng/well). Briefly, apoE was measured using anti-apoE (WuE4) capture antibody, anti-apoE detection antibody (Calbiochem) and an HRP-conjugated secondary antibody. Initially Aβ42 levels were measured in hippocampal extractions from 2, 4 and 6 month old mice (Figure 1) using Wako ELISA kits as previously described (42). All subsequent Aβ42 ELISAs used HJ7.4 as the capture antibody, biotinylated antibody HJ5.1 as the detection antibody and streptavidin-poly-HRP-conjugated secondary antibody, provided by Dr. D. Holtzman (Washington University) (2). For apoE and Aβ42 ELISAs, protein/peptide standards were reconstituted in TBS, TBSX or FA at concentrations equivalent to those in the assayed samples, as appropriate. All data were normalized to the amount of total protein in each extraction sample. For Figures 5, total Aβ or apoE levels in each extraction fraction (i.e. TBS + TBSX + FA) were divided by total protein in each fraction. Oligomeric Aβ (oAβ): oAβ levels were determined based on a modified protocol by Xia and co-workers (24), using the Aβ antibody MOAB-2 (25). MOAB-2 was developed in the LaDu laboratory and is a high-affinity antibody specific for Aβ that does not detect APP. For the oAβ ELISA, MOAB-2 was used as a capture antibody and biotinylated-MOAB-2 as a detection antibody, based on a previous protocol (46). This ELISA pairing detects synthetic oAβ preparations but not monomeric Aβ using preparations of oAβ optimized for the original protocol (data not shown; (46)). These oAβ preparations were used as a standard for measuring soluble oAβ levels in EFAD mice. In addition, the MOAB-2-based oAβ42 ELISA detects oligomeric but not monomeric Aβ42 using synthetic preparations previously characterized by our lab (data not shown; (47,48)).

Thioflavin-S Staining for Plaques

Thio-S plaque staining and quantification was conducted by an investigator blinded to *APOE* genotype using every 9th tissue section for 6 consecutive sections, beginning with the lateral-most section in the region of interest (ROI). Sections were washed in TBS (6 x 5 min), mounted on glass coverslips, allowed to dry, rehydrated in Milli-Q water for 2 min and stained in 0.1% Thio-S (dissolved in 50% EtOH + 50% 1 x PBS) for 5 min in the dark. Tissue was destained in 80% EtOH (2 x 5 min) in the dark and mounted with VectaShield fluorescence mounting media. Quantification of plaque deposition was performed as described (49). Briefly, images were captured on a NanoZoomer slide scanner (Hamamatsu Photonics), exported with NDP viewer software (Hamamatsu Photonics) and converted to 8-bit grayscale using ACDSee Pro 2 software (ACD Systems). Converted images were thresholded to highlight plaques and to diminish background signal (all images were thresholded at the same

Downloaded from www.jbc.org at University of Illinois at Chicago Library, on October 29, 2012

value). Identified objects after thresholding were individually inspected to confirm the object as a plaque. The subiculum and frontal cortex in each image were then outlined and analysed with the "Analyse Particles" function in NIH ImageJ software. Plaques were evaluated for total number and % area covered (total Thio-S immunoreactivity/ROI). Because plaques smaller than 5.5μm were not readily distinguished from background Thio-S fluorescence, limits were set in the ImageJ software such that all plaques greater than 5.5μm were included, and plaques smaller than 5.5μm were excluded.

Plaque Morphology

Preliminary analysis using tissue from EFAD mice indicated that plaques were of three major classifications, consistent with previous descriptions (16,50): 1) Diffuse = no center and weak Thio-S staining with a wispy morphology; 2) Dense-core with halos = obvious center that stains brightly with Thio-S, and a surrounding halo of weakly stained fibrils; 3) Compact = dense-core plaques stain very brightly with Thio-S, appear almost spherical, are generally smaller than plaques with halos and have no obvious halo of fibrils. Quantification of plaque morphology was carried out using every 18th section of subiculum for three consecutive sections as described, using an NIH ImageJ Plugin for a counting application. Total numbers of each plaque type were expressed as a percentage of total plaques counted for each mouse.

Intraneuronal Aβ Counts

The number of neurons containing intraneuronal Aβ was determined using unbiased stereology (51), counted by an investigator blinded to *APOE* genotype using sections immunostained with MOAB-2 (for Aβ) and NeuN. Briefly, every 9th tissue section for 6 consecutive sections was counted beginning with the lateral-most section in which the ROI was first identified. The ROI (subiculum, frontal cortex or CA3) was outlined at 10x magnification using the NeuN fluorescence channel. An optical fractionator design was then used for systematic random sampling of the entire ROI, to make unbiased estimates of total neuronal counts using a three-dimensional optical dissector counting probe. Parameters assume an average mounted tissue thickness of 25μm (to account for tissue shrinkage) with 5μm guard zones, a counting frame size of 200μm x 200μm and an SRS grid size of 300μm x 300μm. Neurons were counted by moving through the entire depth of tissue in both the Aβ and NeuN fluorescence channels at each count site, to ensure the accuracy of intraneuronal Aβ counts (to disqualify extracellular Aβ and/or nonspecific signal). The number of Aβ-containing neurons was calculated by the stereology software based on the above parameters and the measured volume of each ROI, and expressed as the number of neurons per mm^3 of tissue.

Western Blots

Total protein (17.5μg) from TBSX-extracted EFAD cortex was run on 12% Bis-Tris SDS-PAGE gels and transferred to 0.2μm PVDF membrane, followed by overnight incubation in primary antibodies against N-terminal APP (1:2500, Invitrogen) or β-actin as a loading control (1:10,000, Invitrogen). Membranes were washed, incubated in HRP-conjugated secondary antibody raised against mouse IgG, developed with super ECL reagent (Pierce), and exposed using Kodak ImageStation MI software.

Statistical Analyses

Data were analysed by one-way analysis of variance (ANOVA) followed by Tukey's post-hoc analysis (Figure 1B and Figure 6), or by two-way ANOVA followed by Bonferroni post hoc analysis (all other figures) using GraphPad Prism version 4 for Macintosh. $p < 0.05$ was considered significant.

RESULTS

Human *APOE* genotype-specific delay of Aβ accumulation in 5xFAD mice: EFAD transgenic mice

EFAD mice were developed by crossing 5xFAD mice with the three strains of human apoE-TR mice, resulting in E2FAD, E3FAD and E4FAD mice. Given the abundant Aβ pathology in 5xFAD mice at 2 months (11), total Aβ deposition was examined in 2, 4 and 6 month EFAD mice by IHC using the monoclonal anti-Aβ antibody MOAB-2 (Figure 1A), a new anti-Aβ antibody

Downloaded from www.jbc.org at University of Illinois at Chicago Library, on October 29, 2012

that does not recognize full length or soluble APP fragments (25). The overall regional pattern of Aβ accumulation in the brain was similar among the 5xFAD and EFAD mice, with no *APOE* genotype-specific changes. Aβ accumulation appeared first in the subiculum of the hippocampal formation and in the deep layers of the frontal cortex, spreading to the outer layers of the cortex and CA1 region of the hippocampus. Consistent with previous reports (11), 5xFAD mice (expressing endogenous mouse apoE) show extracellular Aβ deposition as early as 2 months that increased with age from 2 to 6 months (Figure 1A). Compared to 5xFAD mice, Aβ deposition is delayed ~4 months in the EFAD mice, with accumulation earliest in E4FAD > E3FAD = E2FAD. Aβ accumulation appeared earlier and was greater in the subiculum compared to the frontal cortex, allowing for regional, as well as temporal, comparisons of the effects of *APOE* genotype on the progression of Aβ accumulation.

To confirm the difference in total Aβ accumulation observed by IHC between 5xFAD and EFAD mice, and among the *APOE* genotypes in the EFAD mice, Aβ42 levels were measured in brain homogenates at 6 months by an Aβ42-specific ELISA (Figure 1B). Consistent with the Aβ accumulation detected by IHC, the levels of total Aβ42 were higher in 5xFAD compared to EFAD mice. Aβ42 levels were highest in E4FAD compared with E2FAD and E3FAD mice. EFAD mice demonstrate *APOE* genotype-dependent changes in Aβ accumulation that are significant in mice aged 2 to 6 months, thus providing a tractable model.

Plaque deposition is greatest in E4FAD, an effect modulated by brain region and *APOE* genotype-specific plaque morphology

Although amyloid plaques may not correlate directly with cognitive decline in AD patients (52), they remain a key determinant in the diagnosis of AD. Importantly, *APOE4* is associated with higher plaque burden than *APOE2* and *APOE3* (53). Therefore, the effect of *APOE* genotype on amyloid plaque burden in the EFAD mice was determined using Thio-S, a stain specific for parallel β-sheet structure (Figure 2). Representative images from 2, 4 and 6 month EFAD mice demonstrate Thio-S staining initiates at 4 months in the subiculum and deep layers of the frontal cortex (Figure 2A) and is increased by 6 months for all *APOE* genotypes, a pattern consistent with IHC for total Aβ (Figure 1A). These data were quantified to determine the number and percent area covered by plaques (frontal cortex-Figure 2B; subiculum-Figure 2C); measures that produced equivalent differences among the *APOE* genotypes. Overall, plaque deposition was greatest in E4FAD mice compared with E2FAD and E3FAD mice, significant at 4 months in the frontal cortex and subiculum, and at 6 months in the frontal cortex.

It is interesting to note that at 6 months in the subiculum, plaque levels in both E2FAD and E4FAD are significantly higher than E3FAD (Figure 2C). Recent reports from the "oldest-of-the-old" studies demonstrate significant plaque burden in the absence of cognitive deficits in *APOE2* subjects (54,55). Importantly, in a case study of an *APOE2/2* subject, plaque morphology was described as fleecy/diffuse compared to the compact/dense-cored morphology of *APOE4* AD patients (15). Based on this potential difference in plaque morphology between the E2FAD and E4FAD mice, plaques in the subiculum (4 and 6 months) were classified and quantified according to the following scale: 1) "Diffuse" = no obvious dense-core; 2) "Dense-cored with halos" = an obvious center with a halo of fibrils; 3) "Compact" = dense-cored plaques that appear spherical (Figure 2D). The majority of the plaques in EFAD mice were either diffuse (1) or compact (3) and this distribution in plaque morphology did not change with age (Figure 2E). In E2FAD and E3FAD mice the majority of plaques were diffuse, accounting for more than 50% of total plaques, while diffuse plaques were significantly lower in E4FAD mice (e.g. 30% at 6 months). The reverse pattern was observed with compact plaques; ~20% of the plaques in E2FAD and E3FAD were compact, while 40-50% of plaques in E4FAD were compact. In addition, from 4 to 6 months, the proportion of diffuse plaques decreased and that of compact plaques increased only in the E4FAD mice (Figure 2E). This trend suggest that *APOE2* and *APOE3* may maintain plaques in a diffuse morphology, whereas *APOE4* facilitates compact plaque formation, the plaque morphology traditionally associated with AD pathology (15).

Downloaded from www.jbc.org at University of Illinois at Chicago Library, on October 29, 2012

Intraneuronal Aβ levels are comparable among the *APOE* genotypes

Intraneuronal Aβ has been observed prior to extracellular plaques in human AD tissue and in mouse models, and has been linked to neurotoxicity (56,57). As previously described, MOAB-2 is an anti-Aβ antibody that specifically detects Aβ, but not APP. MOAB-2 demonstrated strong intraneuronal immunoreactivity in 5xFAD and 3xTg mouse brain tissue that preceded extracellular Aβ deposition (25). To accurately measure the extent of intracellular Aβ accumulation without the confounding contribution of extracellular Aβ deposition, the total number of Aβ-containing neurons were counted in the frontal cortex (Figure 3A for a representative image and B for quantification) and subiculum (Figure 3C) at 2 and 4 months, and the CA3 region of the hippocampus (Figure 3D) at 4 and 6 months using IHC with MOAB-2 and unbiased stereological methods. The number of Aβ-containing neurons increased significantly with time in all three-brain regions (Figure 3B, C and D). However, there were no significant *APOE* genotype-specific differences in the total number of Aβ-containing neurons in any region analysed.

Total apoE levels are lower and total Aβ42 levels are higher in E4FAD mice compared with E2FAD and E3FAD

Total apoE (Figure 4A) and Aβ42 (Figure 4B) levels in 2, 4 and 6-month EFAD mice were measured by ELISAs in the cerebellum (a brain region resistant to Aβ pathology) and the cortex and hippocampus (regions susceptible to Aβ pathology). For IHC, the subiculum was specifically analysed, as it was the region of the hippocampus with the greatest Aβ accumulation. However, for biochemical measurements, it was necessary to homogenize the entire hippocampus, thus "diluting" the subiculum-specific Aβ42 accumulation, although hippocampal Aβ levels remained significantly higher than cortex, as observed with IHC. In general, total apoE4 levels are lower than apoE2 and apoE3, across age and brain region (Figure 4A). Specifically, apoE4 levels are significantly lower than apoE2 and apoE3 in the cerebellum at 4 months, in the cortex at 2, 4, and 6 months, and in the hippocampus at 2 and 4 months old (for specific comparisons, see Figure 4A). Previous publications in humans and mice report lower apoE4 levels compared to apoE3; though little data are published that compare apoE4 levels with apoE2 (3,26,33-35,58,59). Interestingly, total apoE levels in the EFAD mice were lowest in the cerebellum, significantly higher in the cortex, and highest in the hippocampus (Figure 4A; dashed line marks mean the data collapsed by genotype and age within a region, $p < 0.001$). In addition, apoE levels did not change in response to age, thus there was no *APOE* genotype-specific response to increasing Aβ accumulation (Figure 4B).

In the cortex and hippocampus, total Aβ42 levels increased with age in an *APOE* genotype-specific manner (Figure 4B). In the cortex, Aβ42 levels were generally low at 2 months but increased significantly by 4 months such that: E4FAD > E3FAD = E2FAD. It is interesting to note that at 6 months, the levels of Aβ42 in E2FAD and E4FAD were both significantly higher than E3FAD. In the hippocampus, Aβ42 levels were low at 2 months but increased significantly by 4 and 6 months such that: E4FAD > E3FAD = E2FAD. The Aβ42 levels in the cerebellum were below detection until 6 months, when the values were low and equivalent among the genotypes (Figure 4B). As observed for apoE, Aβ42 levels were lowest in the cerebellum, higher in the cortex, and highest in the hippocampus (Figure 4B, $p < 0.001$; note the Y-axis values change for cerebellum and cortex vs. hippocampus). These data in the EFAD mice from 2 to 6 months for total Aβ42 levels are consistent with Aβ immunoreactivity (Figure 1A) and Thio-S staining (Figure 2), demonstrating the earliest accumulation of Aβ in the subiculum followed by the deep layers of the frontal cortex.

In summary, total apoE and Aβ42 levels follow a similar pattern of brain region-dependent accumulation that initiates in the subiculum and the deep layers of the frontal cortex. Total apoE levels do not change in response to age (2-6 months), although apoE4 levels were generally lower than apoE2 and apoE3 at each age and in each brain region. Total Aβ42 levels increase with age in disease susceptible regions, and are generally higher with apoE4 compared with apoE2 and apoE3. Thus, *APOE4* promotes Aβ accumulation in the hippocampus (subiculum) and

Downloaded from www.jbc.org at University of Illinois at Chicago Library, on October 29, 2012

cortex, demonstrated by IHC (Figures 1A), Thio-S staining (Figure 2A) and biochemical analysis (Figure 4).

The lower levels of total apoE4 are the result of a decrease only in the TBSX extraction fraction

Previously, a 3-step extraction protocol was optimized for the detection of apoE and Aβ in the presence of increasing amyloid deposition, particularly focusing on the full extraction of insoluble apoE and Aβ42 with FA, as plaques in the 5xFAD mice are primarily compact/dense-cored (42). Thus, this protocol is a sequential protein extraction in TBS ("soluble"), TBSX ("detergent soluble") and FA ("insoluble"). Figure 5 depicts the extraction profiles for apoE (Figure 5A) and Aβ42 (Figure 5B) from the hippocampus of 2-, 4- and 6-month EFAD mice, as this is the region with the earliest signs of Aβ accumulation (Figures 1, 2 and 4B). In the TBS-soluble fraction, apoE levels did not differ with age or by *APOE* genotype (Figure 5A). ApoE2 and apoE3 extracted primarily to the TBSX fraction, while apoE4 levels were significantly lower in this fraction at 2, 4 and 6 months. In the FA fraction, apoE levels increased from 4 to 6 months with all *APOE* genotypes, consistent with the increase in amyloid plaques (53). The lower total apoE4 levels, compared with total apoE2 and apoE3 (Figure 4A), were reflected primarily in the TBSX fraction of the extraction profile (Figure 5A). Further, the distribution of apoE across the extraction profiles reveals that the proportion of apoE4 in the TBSX fraction is specifically lower in the brain regions susceptible to Aβ pathology (cortex and hippocampus) and not in a region resistant to Aβ pathology (cerebellum) (data not shown). Thus, using an entirely different approach from previous reports, these data provide evidence that the levels of lipoprotein-associated apoE4 are lower than apoE2 and apoE3.

In AD patients, soluble Aβ levels in the brain correlate with disease severity (52). In EFAD mice, Aβ42 increased with age in the TBS-soluble fractions from 2 to 6 months (Figure 5B). At 4 and 6 months, TBS-soluble Aβ42 levels were significantly higher in E4FAD mice compared with E2FAD and E3FAD mice. Indeed, at 6 months, Aβ levels in the E4FAD mice were at least 4-fold higher than E2FAD or E3FAD mice. In the TBSX fractions, Aβ42 did not change significantly with age or *APOE* genotype. FA-extracted Aβ42 levels increased with age for all *APOE* genotypes and were significantly higher in E4FAD mice at 4 and 6 months compared with E2FAD and E3FAD mice (Figure 5B). At 6 months, the Aβ42 levels in the FA fraction of the E4FAD mice were at least 4-fold higher than E2FAD or E3FAD mice, comparable to the difference in the Aβ42 levels in the TBS fraction. The high levels of Aβ42 in the FA fraction of the hippocampus of E4FAD mice is consistent with total Aβ42 levels (Figure 4B), as well as the increased Aβ immunoreactivity (Figure 1A) and Thio-S staining (Figure 2) in the subiculum of the E4FAD mice.

Soluble Aβ42 and soluble oligomeric Aβ levels are higher in E4FAD mice compared with E2FAD and E3FAD mice

Soluble Aβ42 and soluble oAβ are increased in AD patients and are considered important for AD progression (52). However, the effect of *APOE* genotype on these species remains unclear. Therefore, soluble apoE, Aβ42, and oAβ were compared in 6-month EFAD mice (Figure 6). Soluble apoE levels were comparable in the cortex (Figure 6A) and hippocampus (Figure 6B), and did not vary significantly by *APOE* genotype. Therefore, any differences observed in Aβ speciation are likely mediated by differences in the function rather than the amount of each apoE isoform. Soluble Aβ42 levels were higher in the hippocampus than the cortex in EFAD mice (Figure 6), consistent with early Aβ accumulation in this region. Further, in both the hippocampus and cortex, soluble Aβ42 levels were 2-fold higher in the cortex and 3-fold higher in the hippocampus of E4FAD mice compared with E2FAD and E3FAD mice. An ELISA for measuring oAβ was developed using MOAB-2, based on the protocol developed by Xia and co-workers ((24), see details in Methods section). As with soluble Aβ42, oAβ levels were higher in the hippocampus than the cortex. In E4FAD mice, oAβ levels were ~2-fold higher in the cortex and 3-fold higher in the hippocampus compared with E2FAD and E3FAD mice. Thus, Aβ preferentially accumulates as soluble and oligomeric forms in the presence of *APOE4* and, comparing cortex to hippocampus,

Downloaded from www.jbc.org at University of Illinois at Chicago Library, on October 29, 2012

these soluble species of Aβ appear to increase with the accumulation of total Aβ. Overall, these data demonstrate that *APOE* genotype modulates Aβ speciation, an effect likely mediated by functional differences among the apoE-isoforms.

DISCUSSION

In currently available apoE/FAD-Tg mouse models, expression of human *APOE* significantly delays plaque deposition (for review (44)). To generate a more tractable model to investigate the apoE isoform effect on Aβ accumulation, 5xFAD mice (11) were crossed with apoE-TR mice (9) to produce the EFAD mouse model. In 5xFAD mice, neurons produce primarily human Aβ42, and show early and aggressive Aβ42 deposition, with significant intraneuronal Aβ accumulation at 6 weeks, significant plaque deposition at 2 months and subtle changes in synaptic markers at 9 months. ApoE-TR mice are perhaps the most biologically-relevant transgenic mouse model for apoE, as human apoE is expressed primarily by glia at physiologically regulated levels. In EFAD mice, Aβ deposition is delayed ~4 months compared to 5xFAD mice, creating a window from 2 to 6 months during which comparisons of multiple forms of Aβ accumulation can be measured, though still early in the overall process of Aβ accumulation in either the hippocampus or the cortex. Compared with E2FAD and E3FAD mice, E4FAD mice consistently demonstrated accelerated Aβ accumulation, greater total levels of Aβ42, and selective increases in soluble Aβ42 and oAβ levels. Interestingly, rather than simply delaying Aβ accumulation relative to E3FAD, E2FAD mice displayed Aβ accumulation similar to E3FAD. The development of these mice will allow future studies to further probe specific mechanisms for the observed changes among the apoE isoforms, as well as apoE isoform-specific changes in Aβ accumulation.

Autosomal dominant mutations that increase either total Aβ, or specifically Aβ42, cause FAD. However, the identity of the specific assembly(s) of Aβ42 that causes the eventual neurotoxicity characteristic of AD remains unclear. Although total plaque burden does not correlate with the degree of dementia or neurodegenerative pathology in humans (52), plaque staging has identified particular plaque morphologies that likely contribute to neurotoxicity more than others (15,16). Overall, E4FAD mice display the highest plaque load, as expected based on previous studies in humans and transgenic mice (for review (53)). The exception is that the plaque burden in E2FAD mice was equivalent to E4FAD mice in the subiculum at 6 months; the most affected region in the oldest mice studied. However, analysis of plaque morphology revealed that while the majority of the *APOE4* plaques are compact, the majority of the *APOE2* plaques are diffuse. This *APOE2*-induced deposition of diffuse plaques is novel in a mouse model and consistent with the previous work by Dr. C. Kawas and co-workers who reported that increased diffuse plaques are associated with *APOE2* in cognitively normal subjects compared to compact plaques in *APOE4* AD patients from the "Oldest of the old" study (54,55).

The structural properties and composition of different plaque types may correspond to functional differences. A renewed interest in the pathological role of plaques has suggested that oAβ species accumulate at the periphery of dense-core plaques (60,61) and that compact plaques enhance Aβ-toxicity indirectly by creating a platform on which toxic oAβ species can accumulate or stabilize. This effect would be enhanced with *APOE4*, as it is associated with a larger proportion of compact plaques. Diffuse plaques may prevent Aβ-induced toxicity by depriving soluble oAβ of a stable foundation. Determining the effect of *APOE* genotype on the origins, structural characteristics and neurotoxicity of these different plaque types in EFAD mice is a crucial next step.

In addition to plaque morphology, recent evidence indicates that intraneuronal Aβ accumulation may be an important proximal neurotoxic event in AD pathogenesis (for review (56,57)). Indeed, intraneuronal Aβ has been correlated with cognitive deficits in FAD-Tg mice. However, even the existence of Aβ deposits within neurons has recently been challenged by Winton and co-workers (62). These authors purport that it is actually intraneuronal APP being detected by antibodies thought to be specific for Aβ. MOAB-2 is an anti-Aβ antibody that does not detect APP (25). MOAB-2 demonstrates strong intraneuronal

Downloaded from www.jbc.org at University of Illinois at Chicago Library, on October 29, 2012

immunoreactivity in 5xFAD and 3xTg mouse brain tissue that precedes extracellular Aβ deposition. The current study represents one of the first reports of the effects of *APOE* genotype on intraneuronal Aβ in an FAD-Tg mouse model. Using MOAB-2, the accumulation of intraneuronal Aβ was comparable between the isoforms in a specific region at a given age but accumulation increased significantly with age and varied with the AD-susceptibility of the brain region. These data are in apparent contrast with data from a single study in humans that reported an increase in intraneuronal Aβ with 1 or 2 alleles of *APOE4* (63). However, this human study measured Aβ40 while the EFAD mice express almost exclusively Aβ42; one possible explanation for the discrepancy. To our knowledge, no studies have yet reported the effect of *APOE* genotype on intraneuronal Aβ accumulation in an apoE/FAD-Tg mouse.

In E4FAD mice, total apoE levels in the brain are lower compared with E2FAD and E3FAD, as previously observed in human and apoE-Tg mouse models (35-41). With TBS, TBSX and FA extraction, apoE2 and apoE3 from the EFAD mouse tissue extract primarily to the TBSX fraction, consistent with the extraction of apoE-containing lipoproteins from plasma. However, the lower total apoE4 levels are reflected only in their significant reduction in the TBSX fraction, as the levels of apoE2, apoE3 and apoE4 are comparable in the TBS- and FA-extracted fractions. Further, this apoE4-specific distribution appears to occur in the hippocampus and cortex, AD-susceptible brain regions, and not the cerebellum, a disease-resistant region. Because the TBSX fraction contains the apoE extracted specifically from lipoprotein particles, potential interpretations of these data are that less apoE4 is lipoprotein-associated and/or apoE4-containing lipoproteins are less lipidated. Although a substantial amount of research has been devoted to understanding the functional differences between lipidated and non-lipidated apoE, including its ability to bind Aβ (64-69) or apoE receptors (69-72), surprisingly little is known about the effect of apoE-isoform on the lipidation state of CNS-relevant lipoproteins. Although general dogma in the field is that apoE4 is less lipidated than apoE3, the number of publications that compare the lipidation state of apoE4-particles to apoE3-particles *in vivo* is severely limited. Relevant *in vitro* data include, for example, the results that glial-mediated degradation of apoE4 is increased and cholesterol release is reduced in primary glial cultures from apoE-TR mice expressing apoE4, compared to glial cells expressing apoE3 (73) (39). Thus, the extraction profiles for the apoE isoforms, as presented in this manuscript, will provide critical, novel information for interpreting results from AD therapeutics that target apoE levels and/or its level of lipidation (74-77).

The neurotoxicity of soluble oAβ is of interest because of the apparent correlation of oAβ levels with disease severity: soluble oligomers correlate with cognitive decline (MMSE scores) and tangle stage (20). In FAD-Tg mice, soluble oAβ suppresses synaptic function, reduces synaptic plasticity and impairs learning and memory (52). Prior work from our lab demonstrates that oAβ-induced deficits in synaptic plasticity (78) and neuronal viability (79) are enhanced in the presence of *APOE4* compared with *APOE2* and *APOE3*. The current work illustrates that soluble Aβ42 and oAβ levels are increased in the TBS-soluble fractions of the disease-vulnerable cortex and hippocampus in the E4FAD mice, and the preferential accumulation of Aβ42 results in an increase in both oAβ and plaques. As discussed above, the *APOE4*-specific increase in compact plaques formation may provide a platform for the assembly of oAβ.

The apoE isoform-specific effects on soluble species of Aβ continues to be the focus of extensive research efforts, and a number of potential molecular mechanisms have been proposed. These include effects on: Aβ oligomerization (80,81), Aβ clearance though multiple mechanisms including intracellular uptake and degradation by glia (82-85) and neurons (86,87), clearance across the BBB (88,89), extracellular enzymatic degradation (64), ISF-mediated clearance (90), and perivascular drainage (91), in addition to the potential interplay between plaque morphology, apoE and oAβ levels (for example (92)). Further, whether these effects are mediated by direct binding of Aβ to apoE (68) or by apoE-specific pathways and receptors add further layers of complexity (76).

Downloaded from www.jbc.org at University of Illinois at Chicago Library, on October 29, 2012

Modulating the levels of apoE is an attractive target for AD therapy. Indeed, recent evidence demonstrated that bexarotene (BEX, an RXR agonist) increased apoE levels and decreased soluble Aβ in mice within hours and significantly reduced insoluble Aβ after three days, although plaque levels at 3 months were unchanged (76). However, application of these data to AD patients is difficult as this initial study used transgenic mice producing human Aβ but expressing mouse apoE. Therefore, it is important to demonstrate drug efficacy on Aβ pathology, and in particular Aβ speciation, in FAD-Tg mice that express the human apoE isoforms prior to clinical trial initiation. Although drug intervention trials have not yet been performed on the EFAD mice, these mice are a model of early Aβ pathology, express the human apoE isoforms, demonstrate apoE isoform-specific effects on early Aβ speciation and are thus an ideal model for efficient evaluation of drug therapies targeting apoE. In addition, initial therapeutic testing in a transgenic mouse expressing the human apoE isoforms is critical as *APOE4* carriers can exhibit a differential response to certain therapeutic interventions, complicating interpretation of drug trials that can lead to costly failure after extensive Phase 3 clinical trials (53).

In conclusion, EFAD mice represent a tractable new mouse model that allowed the identification of the *APOE* genotype effects on the earliest accumulations of Aβ (from 2 to 6 months). While *APOE* genotype-specific differences were observed in plaque deposition and morphology, intraneuronal Aβ deposition was not apoE isoform-specific. Compared with *APOE2* and *APOE3*, *APOE4* promoted higher levels of total Aβ42, as well as soluble Aβ42 and oAβ. In addition, the levels of apoE4 are lower and less apoE4 appears to be lipoprotein-associated compared with apoE2 or apoE3. Thus, a number of apoE isoform-specific mechanisms were identified *in vivo* that likely contribute to the effect of *APOE* genotype on AD risk. EFAD mice can be used for further study of these mechanisms. These mice may also provide a model for the efficient evaluation of both AD drug prevention and treatment paradigms. The risk imparted by *APOE4* extends to other cerebral insults with amyloid deposition, including traumatic brain injury, cerebral haemorrhage, and stroke, suggesting that EFAD mice may also provide a model to assess a additional therapeutic strategies.

REFERENCES

1. Bu, G. (2009) Apolipoprotein E and its receptors in Alzheimer's disease: pathways, pathogenesis and therapy. *Nat Rev Neurosci* **10**, 333-344
2. Kim, J., Jiang, H., Park, S., Eltorai, A. E., Stewart, F. R., Yoon, H., Basak, J. M., Finn, M. B., and Holtzman, D. M. (2011) Haploinsufficiency of human APOE reduces amyloid deposition in a mouse model of amyloid-beta amyloidosis. *J Neurosci* **31**, 18007-18012
3. Bales, K. R., Liu, F., Wu, S., Lin, S., Koger, D., DeLong, C., Hansen, J. C., Sullivan, P. M., and Paul, S. M. (2009) Human APOE isoform-dependent effects on brain beta-amyloid levels in PDAPP transgenic mice. *The Journal of neuroscience* **29**, 6771-6779
4. Drzezga, A., Grimmer, T., Henriksen, G., Muhlau, M., Perneczky, R., Miederer, I., Praus, C., Sorg, C., Wohlschlager, A., Riemenschneider, M., Wester, H. J., Foerstl, H., Schwaiger, M., and Kurz, A. (2009) Effect of APOE genotype on amyloid plaque load and gray matter volume in Alzheimer disease. *Neurology* **72**, 1487-1494
5. Grimmer, T., Tholen, S., Yousefi, B. H., Alexopoulos, P., Forschler, A., Forstl, H., Henriksen, G., Klunk, W. E., Mathis, C. A., Perneczky, R., Sorg, C., Kurz, A., and Drzezga, A. (2010) Progression of cerebral amyloid load is associated with the apolipoprotein E epsilon4 genotype in Alzheimer's disease. *Biol Psychiatry* **68**, 879-884
6. Buttini, M., Yu, G. Q., Shockley, K., Huang, Y., Jones, B., Masliah, E., Mallory, M., Yeo, T., Longo, F. M., and Mucke, L. (2002) Modulation of Alzheimer-like synaptic and

Downloaded from www.jbc.org at University of Illinois at Chicago Library, on October 29, 2012

cholinergic deficits in transgenic mice by human apolipoprotein E depends on isoform, aging, and overexpression of amyloid beta peptides but not on plaque formation. *J Neurosci* **22**, 10539-10548

7. Holtzman, D. M., Bales, K. R., Tenkova, T., Fagan, A. M., Parsadanian, M., Sartorius, L. J., Mackey, B., Olney, J., McKeel, D., Wozniak, D., and Paul, S. M. (2000) Apolipoprotein E isoform-dependent amyloid deposition and neuritic degeneration in a mouse model of Alzheimer's disease. *Proc Natl Acad Sci U S A* **97**, 2892-2897
8. Fryer, J. D., Simmons, K., Parsadanian, M., Bales, K. R., Paul, S. M., Sullivan, P. M., and Holtzman, D. M. (2005) Human apolipoprotein E4 alters the amyloid-beta 40:42 ratio and promotes the formation of cerebral amyloid angiopathy in an amyloid precursor protein transgenic model. *J Neurosci* **25**, 2803-2810
9. Sullivan, P. M., Mezdour, H., Aratani, Y., Knouff, C., Najib, J., Reddick, R. L., Quarfordt, S. H., and Maeda, N. (1997) Targeted replacement of the mouse apolipoprotein E gene with the common human APOE3 allele enhances diet-induced hypercholesterolemia and atherosclerosis. *J Biol Chem* **272**, 17972-17980
10. Games, D., Adams, D., Alessandrini, R., Barbour, R., Berthelette, P., Blackwell, C., Carr, T., Clemens, J., Donaldson, T., Gillespie, F., Guido, T., Hagopian, S., Johnson-Wood, K., Khan, K., Lee, M., Leibowitz, P., Lieberburg, I., Little, S., Masliah, E., McConlogue, L., Montoya-Zavala, Mucke, L., Paganini, L., Penniman, E., Power, M., Schenk, D., Seubert, P., Snyder, B., Soriano, F., Tan, H., Vitale, J., Wadsworth, S., Wolozin, B., and Zhao, J. (1995) Alzheimer-type neuropathology in transgenic mice overexpressing V717F ß-amyloid precursor protein. *Nature* **373**, 523-527
11. Oakley, H., Cole, S. L., Logan, S., Maus, E., Shao, P., Craft, J., Guillozet-Bongaarts, A., Ohno, M., Disterhoft, J., Van Eldik, L., Berry, R., and Vassar, R. (2006) Intraneuronal beta-amyloid aggregates, neurodegeneration, and neuron loss in transgenic mice with five familial Alzheimer's disease mutations: potential factors in amyloid plaque formation. *J Neurosci* **26**, 10129-10140
12. Fernandez-Vizarra, P., Fernandez, A. P., Castro-Blanco, S., Serrano, J., Bentura, M. L., Martinez-Murillo, R., Martinez, A., and Rodrigo, J. (2004) Intra- and extracellular Abeta and PHF in clinically evaluated cases of Alzheimer's disease. *Histol Histopathol* **19**, 823-844
13. D'Andrea, M. R., Nagele, R. G., Wang, H. Y., and Lee, D. H. (2002) Consistent immunohistochemical detection of intracellular beta-amyloid42 in pyramidal neurons of Alzheimer's disease entorhinal cortex. *Neurosci Lett* **333**, 163-166
14. D'Andrea, M. R., Nagele, R. G., Wang, H. Y., Peterson, P. A., and Lee, D. H. (2001) Evidence that neurones accumulating amyloid can undergo lysis to form amyloid plaques in Alzheimer's disease. *Histopathology* **38**, 120-134
15. Thal, D. R., Griffin, W. S., and Braak, H. (2008) Parenchymal and vascular Abeta-deposition and its effects on the degeneration of neurons and cognition in Alzheimer's disease. *Journal of cellular and molecular medicine* **12**, 1848-1862
16. Thal, D. R., Capetillo-Zarate, E., Del Tredici, K., and Braak, H. (2006) The development of amyloid beta protein deposits in the aged brain. *Sci Aging Knowledge Environ* **2006**, re1
17. Haass, C., and Selkoe, D. J. (2007) Soluble protein oligomers in neurodegeneration: lessons from the Alzheimer's amyloid beta-peptide. *Nat Rev Mol Cell Biol* **8**, 101-112

Downloaded from www.jbc.org at University of Illinois at Chicago Library, on October 29, 2012

18. Kuo, Y. M., Emmerling, M. R., Vigo-Pelfrey, C., Kasunic, T. C., Kirkpatrick, J. B., Murdoch, G. H., Ball, M. J., and Roher, A. E. (1996) Water-soluble Abeta (N-40, N-42) oligomers in normal and Alzheimer disease brains. *J. Biol. Chem.* **271**, 4077-4081
19. Selkoe, D. J. (2011) Resolving controversies on the path to Alzheimer's therapeutics. *Nat Med* **17**, 1060-1065
20. Tomic, J. L., Pensalfini, A., Head, E., and Glabe, C. G. (2009) Soluble fibrillar oligomer levels are elevated in Alzheimer's disease brain and correlate with cognitive dysfunction. *Neurobiology of disease* **35**, 352-358
21. Jin, M., Shepardson, N., Yang, T., Chen, G., Walsh, D., and Selkoe, D. J. (2011) Soluble amyloid beta-protein dimers isolated from Alzheimer cortex directly induce Tau hyperphosphorylation and neuritic degeneration. *Proc Natl Acad Sci U S A* **108**, 5819-5824
22. McLean, C. A., Cherny, R. A., Fraser, F. W., Fuller, S. J., Smith, M. J., Beyreuther, K., Bush, A. I., and Masters, C. L. (1999) Soluble pool of Abeta amyloid as a determinant of severity of neurodegeneration in Alzheimer's disease. *Ann Neurol* **46**, 860-866
23. Huang, Y., and Mucke, L. (2012) Alzheimer mechanisms and therapeutic strategies. *Cell* **148**, 1204-1222
24. Xia, W., Yang, T., Shankar, G., Smith, I. M., Shen, Y., Walsh, D. M., and Selkoe, D. J. (2009) A specific enzyme-linked immunosorbent assay for measuring beta-amyloid protein oligomers in human plasma and brain tissue of patients with Alzheimer disease. *Arch Neurol* **66**, 190-199
25. Youmans, K. L., Tai, L. M., Kanekiyo, T., Stine, W. B., Jr., Michon, S. C., Nwabuisi-Heath, E., Manelli, A., Fu, Y., Riordan, S., Eimer, W. A., Binder, L., Bu, G., Yu, C., Hartley, D. M., and Ladu, M. J. (2012) Intraneuronal Abeta detection in 5xFAD mice by a new Abeta-specific antibody. *Mol Neurodegener* **7**, 8
26. Poirier, J. (2005) Apolipoprotein E, cholesterol transport and synthesis in sporadic Alzheimer's disease. *Neurobiol Aging* **26**, 355-361
27. Poirier, J. (2008) Apolipoprotein E represents a potent gene-based therapeutic target for the treatment of sporadic Alzheimer's disease. *Alzheimers Dement* **4**, S91-97
28. Ramaswamy, G., Xu, Q., Huang, Y., and Weisgraber, K. H. (2005) Effect of domain interaction on apolipoprotein E levels in mouse brain. *J Neurosci* **25**, 10658-10663
29. Raffai, R. L., Dong, L. M., Farese, R. V., Jr., and Weisgraber, K. H. (2001) Introduction of human apolipoprotein E4 "domain interaction" into mouse apolipoprotein E. *Proc Natl Acad Sci U S A* **98**, 11587-11591.
30. Bertrand, P., Poirier, J., Oda, T., Finch, C. E., and Pasinetti, G. M. (1995) Association of apolipoprotein E genotype with brain levels of apolipoprotein E and apolipoprotein J (clusterin) in Alzheimer disease. *Brain Res Mol Brain Res* **33**, 174-178
31. Glockner, F., Meske, V., and Ohm, T. G. (2002) Genotype-related differences of hippocampal apolipoprotein E levels only in early stages of neuropathological changes in Alzheimer's disease. *Neuroscience* **114**, 1103-1114
32. Cruchaga, C., Kauwe, J. S., Nowotny, P., Bales, K., Pickering, E. H., Mayo, K., Bertelsen, S., Hinrichs, A., Fagan, A. M., Holtzman, D. M., Morris, J. C., and Goate, A. M. (2012) Cerebrospinal fluid APOE levels: an endophenotype for genetic studies for Alzheimer's disease. *Hum Mol Genet*
33. Beffert, U., Cohn, J. S., Petit-Turcotte, C., Tremblay, M., Aumont, N., Ramassamy, C., Davignon, J., and Poirier, J. (1999) Apolipoprotein E and beta-amyloid levels in the

Downloaded from www.jbc.org at University of Illinois at Chicago Library, on October 29, 2012

hippocampus and frontal cortex of Alzheimer's disease subjects are disease-related and apolipoprotein E genotype dependent. *Brain Res* **843**, 87-94
34. Sullivan, P. M., Han, B., Liu, F., Mace, B. E., Ervin, J. F., Wu, S., Koger, D., Paul, S., and Bales, K. R. (2011) Reduced levels of human apoE4 protein in an animal model of cognitive impairment. *Neurobiol Aging* **32**, 791-801
35. Riddell, D. R., Zhou, H., Atchison, K., Warwick, H. K., Atkinson, P. J., Jefferson, J., Xu, L., Aschmies, S., Kirksey, Y., Hu, Y., Wagner, E., Parratt, A., Xu, J., Li, Z., Zaleska, M. M., Jacobsen, J. S., Pangalos, M. N., Reinhart, P. H., Riddell, D. R., Zhou, H., Atchison, K., Warwick, H. K., Atkinson, P. J., Jefferson, J., Xu, L., Aschmies, S., Kirksey, Y., Hu, Y., Wagner, E., Parratt, A., Xu, J., Li, Z., Zaleska, M. M., Jacobsen, J. S., Pangalos, M. N., and Reinhart, P. H. (2008) Impact of apolipoprotein E (ApoE) polymorphism on brain ApoE levels. *Journal of Neuroscience* **28**, 11445-11453
36. Cushley, R. J., and Okon, M. (2002) NMR studies of lipoprotein structure. *Annu Rev Biophys Biomol Struct* **31**, 177-206
37. Gangabadage, C. S., Zdunek, J., Tessari, M., Nilsson, S., Olivecrona, G., and Wijmenga, S. S. (2008) Structure and dynamics of human apolipoprotein CIII. *J Biol Chem* **283**, 17416-17427
38. Krul, E. S., and Cole, T. G. (1996) Quantitation of apolipoprotein E. *Methods Enzymol* **263**, 170-187
39. Riddell, D. R., Zhou, H., Atchison, K., Warwick, H. K., Atkinson, P. J., Jefferson, J., Xu, L., Aschmies, S., Kirksey, Y., Hu, Y., Wagner, E., Parratt, A., Xu, J., Li, Z., Zaleska, M. M., Jacobsen, J. S., Pangalos, M. N., and Reinhart, P. H. (2008) Impact of apolipoprotein E (ApoE) polymorphism on brain ApoE levels. *J Neurosci* **28**, 11445-11453
40. Krul, E., and Cole, T. (1996) Quantitation of apolipoprotein E. in *Methods in Enzymology*, Academic Press, New York. pp 170-187
41. Wang, N., Weng, W., Breslow, J. L., and Tall, A. R. (1996) Scavenger receptor BI (SR-BI) is up-regulated in adrenal gland in apolipoprotein A-I and hepatic lipase knock-out mice as a response to depletion of cholesterol stores. In vivo evidence that SR-BI is a functional high density lipoprotein receptor under feedback control. *J Biol Chem* **271**, 21001-21004
42. Youmans, K. L., Leung, S., Zhang, J., Maus, E., Baysac, K., Bu, G., Vassar, R., Yu, C., and Ladu, M. J. (2011) Amyloid-beta42 alters apolipoprotein E solubility in brains of mice with five familial AD mutations. *J Neurosci Methods* **196**, 51-59
43. Sullivan, P. M., Mezdour, H., Quarfordt, S. H., and Maeda, N. (1998) Type III hyperlipoproteinemia and spontaneous atherosclerosis in mice resulting from gene replacement of mouse Apoe with human Apoe*2. *J Clin Invest* **102**, 130-135
44. Tai, L. M., Youmans, K. L., Jungbauer, L., Yu, C., and Ladu, M. J. (2011) Introducing Human APOE into Abeta Transgenic Mouse Models. *Int J Alzheimers Dis* **2011**, 810981
45. Bien-Ly, N., Gillespie, A. K., Walker, D., Yoon, S. Y., and Huang, Y. (2012) Reducing human apolipoprotein e levels attenuates age-dependent abeta accumulation in mutant human amyloid precursor protein transgenic mice. *J Neurosci* **32**, 4803-4811
46. Moore, B. D., Rangachari, V., Tay, W. M., Milkovic, N. M., and Rosenberry, T. L. (2009) Biophysical analyses of synthetic amyloid-beta(1-42) aggregates before and after covalent cross-linking. Implications for deducing the structure of endogenous amyloid-beta oligomers. *Biochemistry* **48**, 11796-11806

Downloaded from www.jbc.org at University of Illinois at Chicago Library, on October 29, 2012

47. Dahlgren, K. N., Manelli, A. M., Stine, W. B., Jr., Baker, L. K., Krafft, G. A., and LaDu, M. J. (2002) Oligomeric and fibrillar species of amyloid-beta peptides differentially affect neuronal viability. *J Biol Chem* **277**, 32046-32053
48. Stine, W. B., Jr., Dahlgren, K. N., Krafft, G. K., and LaDu, M. J. (2003) In vitro characterization of conditions for amyloid-beta peptide oligomerization and fibrillogenesis. *J Biol Chem* **278**, 11612-11622
49. Kim, D., and Tsai, L. H. (2009) Bridging physiology and pathology in AD. *Cell* **137**, 997-1000
50. Fiala, J. C. (2007) Mechanisms of amyloid plaque pathogenesis. *Acta Neuropathol* **114**, 551-571
51. West, M. J., Slomianka, L., and Gundersen, H. J. (1991) Unbiased stereological estimation of the total number of neurons in thesubdivisions of the rat hippocampus using the optical fractionator. *Anat Rec* **231**, 482-497
52. Larson, M. E., and Lesne, S. E. (2012) Soluble Abeta oligomer production and toxicity. *J Neurochem* **120 Suppl 1**, 125-139
53. Verghese, P. B., Castellano, J. M., and Holtzman, D. M. (2011) Apolipoprotein E in Alzheimer's disease and other neurological disorders. *Lancet Neurol* **10**, 241-252
54. Berlau, D. J., Corrada, M. M., Head, E., and Kawas, C. H. (2009) APOE epsilon2 is associated with intact cognition but increased Alzheimer pathology in the oldest old. *Neurology* **72**, 829-834
55. Berlau, D. J., Kahle-Wrobleski, K., Head, E., Goodus, M., Kim, R., and Kawas, C. (2007) Dissociation of neuropathologic findings and cognition: case report of an apolipoprotein E epsilon2/epsilon2 genotype. *Arch Neurol* **64**, 1193-1196
56. Gouras, G. K., Tampellini, D., Takahashi, R. H., and Capetillo-Zarate, E. (2010) Intraneuronal beta-amyloid accumulation and synapse pathology in Alzheimer's disease. *Acta neuropathologica* **119**, 523-541
57. Bayer, T. A., and Wirths, O. (2010) Intracellular accumulation of amyloid-Beta - a predictor for synaptic dysfunction and neuron loss in Alzheimer's disease. *Front Aging Neurosci* **2**, 8
58. Sullivan, P. M., Mace, B. E., Maeda, N., and Schmechel, D. E. (2004) Marked regional differences of brain human apolipoprotein E expression in targeted replacement mice. *Neuroscience* **124**, 725-733
59. Vitek, M. P., Brown, C. M., and Colton, C. A. (2009) APOE genotype-specific differences in the innate immune response. *Neurobiol Aging* **30**, 1350-1360
60. Koffie, R. M., Meyer-Luehmann, M., Hashimoto, T., Adams, K. W., Mielke, M. L., Garcia-Alloza, M., Micheva, K. D., Smith, S. J., Kim, M. L., Lee, V. M., Hyman, B. T., and Spires-Jones, T. L. (2009) Oligomeric amyloid beta associates with postsynaptic densities and correlates with excitatory synapse loss near senile plaques. *Proceedings of the National Academy of Sciences of the United States of America* **106**, 4012-4017
61. Spires-Jones, T. L., Calignon, A., Meyer-Luehmann, M., Bacskai, B. J., and Hyman, B. T. (2011) Monitoring protein aggregation and toxicity in Alzheimer's disease mouse models using in vivo imaging. *Methods* **53**, 201-207
62. Winton, M. J., Lee, E. B., Sun, E., Wong, M. M., Leight, S., Zhang, B., Trojanowski, J. Q., and Lee, V. M. (2011) Intraneuronal APP, Not Free A{beta} Peptides in 3xTg-AD Mice: Implications for Tau versus A{beta}-Mediated Alzheimer Neurodegeneration. *J Neurosci* **31**, 7691-7699

Downloaded from www.jbc.org at University of Illinois at Chicago Library, on October 29, 2012

63. Christensen, D. Z., Schneider-Axmann, T., Lucassen, P. J., Bayer, T. A., and Wirths, O. (2010) Accumulation of intraneuronal Abeta correlates with ApoE4 genotype. *Acta Neuropathol* **119**, 555-566
64. Jiang, Q., Lee, C. Y., Mandrekar, S., Wilkinson, B., Cramer, P., Zelcer, N., Mann, K., Lamb, B., Willson, T. M., Collins, J. L., Richardson, J. C., Smith, J. D., Comery, T. A., Riddell, D., Holtzman, D. M., Tontonoz, P., and Landreth, G. E. (2008) ApoE promotes the proteolytic degradation of Abeta. *Neuron* **58**, 681-693
65. Hirsch-Reinshagen, V., Maia, L. F., Burgess, B. L., Blain, J. F., Naus, K. E., McIsaac, S. A., Parkinson, P. F., Chan, J. Y., Tansley, G. H., Hayden, M. R., Poirier, J., Van Nostrand, W., and Wellington, C. L. (2005) The absence of ABCA1 decreases soluble apoE levels but does not diminish amyloid deposition in two murine models of Alzheimer's disease. *J Biol Chem* **280**, 43243-43256
66. LaDu, M. J., Falduto, M. T., Manelli, A. M., Reardon, C. A., Getz, G. S., and Frail, D. E. (1994) Isoform-specific binding of apolipoprotein E to beta-amyloid. *J Biol Chem* **269**, 23403-23406
67. LaDu, M. J., Lukens, J. R., Reardon, C. A., and Getz, G. S. (1997) Association of human, rat, and rabbit apolipoprotein E with beta-amyloid. *J Neurosci Res* **49**, 9-18
68. LaDu, M. J., Munson, G. W., Jungbauer, L., Getz, G. S., Reardon, C. A., Tai, L. M., and Yu, C. (2012) Preferential interactions between ApoE-containing lipoproteins and Abeta revealed by a detection method that combines size exclusion chromatography with non-reducing gel-shift. *Biochim Biophys Acta - Molecular and Cell Biology of Lipids* **1821**, 295-302
69. LaDu, M. J., Stine, W. B., Jr., Narita, M., Getz, G. S., Reardon, C. A., and Bu, G. (2006) Self-Assembly of HEK Cell-Secreted ApoE Particles Resembles ApoE Enrichment of Lipoproteins as a Ligand for the LDL Receptor-Related Protein. *Biochemistry* **45**, 381-390
70. Manelli, A. M., Stine, W. B., Van Eldik, L. J., and LaDu, M. J. (2004) ApoE and Abeta1-42 interactions: effects of isoform and conformation on structure and function. *J Mol Neurosci* **23**, 235-246
71. Holtzman, D. M., Herz, J., and Bu, G. (2012) Apolipoprotein e and apolipoprotein e receptors: normal biology and roles in Alzheimer disease. *Cold Spring Harb Perspect Med* **2**, a006312
72. Hauser, P. S., Narayanaswami, V., and Ryan, R. O. (2011) Apolipoprotein E: from lipid transport to neurobiology. *Prog Lipid Res* **50**, 62-74
73. Gong, J. S., Kobayashi, M., Hayashi, H., Zou, K., Sawamura, N., Fujita, S. C., Yanagisawa, K., and Michikawa, M. (2002) Apolipoprotein E (apoE) isoform-dependent lipid release from astrocytes prepared from human-apoE3- and apoE4-knock-in mice. *J Biol Chem* **31**, 31
74. Wang, H., Durham, L., Dawson, H., Song, P., Warner, D. S., Sullivan, P. M., Vitek, M. P., and Laskowitz, D. T. (2007) An apolipoprotein E-based therapeutic improves outcome and reduces Alzheimer's disease pathology following closed head injury: evidence of pharmacogenomic interaction. *Neuroscience* **144**, 1324-1333
75. Sadowski, M. J., Pankiewicz, J., Scholtzova, H., Mehta, P. D., Prelli, F., Quartermain, D., and Wisniewski, T. (2006) Blocking the apolipoprotein E/amyloid-beta interaction as a potential therapeutic approach for Alzheimer's disease. *Proceedings of the National Academy of Sciences of the United States of America* **103**, 18787-18792

Downloaded from www.jbc.org at University of Illinois at Chicago Library, on October 29, 2012

76. Cramer, P. E., Cirrito, J. R., Wesson, D. W., Lee, C. Y., Karlo, J. C., Zinn, A. E., Casali, B. T., Restivo, J. L., Goebel, W. D., James, M. J., Brunden, K. R., Wilson, D. A., and Landreth, G. E. (2012) ApoE-directed therapeutics rapidly clear beta-amyloid and reverse deficits in AD mouse models. *Science* **335**, 1503-1506
77. Mahley, R. W., Weisgraber, K. H., and Huang, Y. (2006) Apolipoprotein E4: a causative factor and therapeutic target in neuropathology, including Alzheimer's disease. *Proceedings of the National Academy of Sciences of the United States of America* **103**, 5644-5651
78. Trommer, B. L., Shah, C., Yun, S. H., Gamkrelidze, G., Pasternak, E. S., Stine, W. B., Manelli, A., Sullivan, P., Pasternak, J. F., and LaDu, M. J. (2005) ApoE isoform-specific effects on LTP: blockade by oligomeric amyloid-beta1-42. *Neurobiology of disease* **18**, 75-82
79. Manelli, A. M., Bulfinch, L. C., Sullivan, P. M., and LaDu, M. J. (2007) Abeta42 neurotoxicity in primary co-cultures: effect of apoE isoform and Abeta conformation. *Neurobiol Aging* **28**, 1139-1147
80. Cerf, E., Gustot, A., Goormaghtigh, E., Ruysschaert, J. M., and Raussens, V. (2011) High ability of apolipoprotein E4 to stabilize amyloid-{beta} peptide oligomers, the pathological entities responsible for Alzheimer's disease. *FASEB J*
81. Petrlova, J., Hong, H. S., Bricarello, D. A., Harishchandra, G., Lorigan, G. A., Jin, L. W., and Voss, J. C. (2011) A differential association of Apolipoprotein E isoforms with the amyloid-beta oligomer in solution. *Proteins* **79**, 402-416
82. Koistinaho, M., Lin, S., Wu, X., Esterman, M., Koger, D., Hanson, J., Higgs, R., Liu, F., Malkani, S., Bales, K. R., and Paul, S. M. (2004) Apolipoprotein E promotes astrocyte colocalization and degradation of deposited amyloid-beta peptides. *Nat Med* **10**, 719-726
83. Mandrekar, S., Jiang, Q., Lee, C. Y., Koenigsknecht-Talboo, J., Holtzman, D. M., and Landreth, G. E. (2009) Microglia mediate the clearance of soluble Abeta through fluid phase macropinocytosis. *J Neurosci* **29**, 4252-4262
84. Basak, J. M., Verghese, P. B., Yoon, H., Kim, J., and Holtzman, D. M. (2012) Low-density lipoprotein receptor represents an apolipoprotein E-independent pathway of Abeta uptake and degradation by astrocytes. *J Biol Chem* **287**, 13959-13971
85. Thal, D. R. (2012) The role of astrocytes in amyloid beta-protein toxicity and clearance. *Exp Neurol* **236**, 1-5
86. Vekrellis, K., Ye, Z., Qiu, W. Q., Walsh, D., Hartley, D., Chesneau, V., Rosner, M. R., and Selkoe, D. J. (2000) Neurons regulate extracellular levels of amyloid beta-protein via proteolysis by insulin-degrading enzyme. *Journal of Neuroscience* **20**, 1657-1665
87. Wirths, O., and Bayer, T. A. (2012) Intraneuronal Abeta accumulation and neurodegeneration: Lessons from transgenic models. *Life Sci*
88. Deane, R., Sagare, A., Hamm, K., Parisi, M., Lane, S., Finn, M. B., Holtzman, D. M., and Zlokovic, B. V. (2008) apoE isoform-specific disruption of amyloid beta peptide clearance from mouse brain. *J Clin Invest* **118**, 4002-4013
89. Bachmeier, C., Beaulieu-Abdelahad, D., Crawford, F., Mullan, M., and Paris, D. (2012) Stimulation of the Retinoid X Receptor Facilitates Beta-Amyloid Clearance Across the Blood-Brain Barrier. *J Mol Neurosci*
90. Castellano, J. M., Kim, J., Stewart, F. R., Jiang, H., DeMattos, R. B., Patterson, B. W., Fagan, A. M., Morris, J. C., Mawuenyega, K. G., Cruchaga, C., Goate, A. M., Bales, K.

Downloaded from www.jbc.org at University of Illinois at Chicago Library, on October 29, 2012

R., Paul, S. M., Bateman, R. J., and Holtzman, D. M. (2011) Human apoE isoforms differentially regulate brain amyloid-beta peptide clearance. *Sci Transl Med* **3**, 89ra57

91. Hawkes, C. A., Sullivan, P. M., Hands, S., Weller, R. O., Nicoll, J. A., and Carare, R. O. (2012) Disruption of Arterial Perivascular Drainage of Amyloid-beta from the Brains of Mice Expressing the Human APOE epsilon4 Allele. *PLoS One* **7**, e41636

92. Jones, P. B., Adams, K. W., Rozkalne, A., Spires-Jones, T. L., Hshieh, T. T., Hashimoto, T., von Armin, C. A., Mielke, M., Bacskai, B. J., and Hyman, B. T. (2011) Apolipoprotein E: isoform specific differences in tertiary structure and interaction with amyloid-beta in human Alzheimer brain. *PLoS One* **6**, e14586

FOOTNOTES

[1] **Abbreviations:** AD, Alzheimer's disease; Aβ, amyloid-β; apoE, apolipoprotein E; APP, amyloid precursor protein; FAD, familial-AD; FAD-Tg, transgenic mice expressing APP and/or PS1 with FAD mutations; apoE-TR, apoE targeted replacement mice; 5xFAD mice, mice expressing 5 FAD mutations; EFAD mice, 5xFAD mice crossed with apoE-TR mice; oAβ, oligomeric Aβ; Cx, cortex; H, hippocampus, CB, cerebellum; PFA, paraformaldehyde; TBSX, TBS containing 1% Triton X-100 FA, formic acid; Thio-S, thioflavin S.

FIGURE LEGENDS

Figure 1. Human *APOE* genotype-specific delay of Aβ accumulation in 5xFAD mice: EFAD transgenic mice. (A) Representative images of sagittal brain sections of 2, 4 and 6 month 5xFAD and EFAD mice immunostained for Aβ (red) and NeuN (green), 20x magnification (scale bar = 500μm). **(B)** Total Aβ42 levels in the hippocampus of 6-month 5xFAD and EFAD mice measured by ELISA. Data are expressed as mean ± SEM and were analysed by one-way ANOVA followed by Tukey's multiple comparison post-hoc analysis. $^{*}p < 0.05$ vs. m-apoE, $^{\#}p < 0.05$ vs. apoE2 and apoE3.

Figure 2. Plaque deposition is greatest in E4FAD, an effect modulated by brain region and *APOE* genotype-specific plaque morphology. (A) Representative images of sagittal brain sections from 2, 4 and 6 month EFAD mice stained with Thio-S (green), 20x magnification (scale bar = 500μm). Quantification of the number of plaques and % area covered by plaques in the **(B)** frontal cortex and **(C)** subiculum. **(D)** Plaque Morphology: representative images of the primary types of plaques in EFAD brain, 63x magnification: diffuse, dense-cored with halos, and compact (scale bar = 20μm). **(E)** Quantification of plaque morphology in subiculum: percentage of each plaque type in 4- and 6-month EFAD mice. Data are expressed as mean ± SEM and were analysed by two-way ANOVA followed by Bonferroni multiple comparison post hoc analysis. $^{*}p < 0.05$ vs. 2 or 4 months, $^{\#}p < 0.05$ vs. apoE2 and apoE3, $^{\ddagger}p < 0.05$ vs. apoE3.

Figure 3. Intraneuronal Aβ levels are comparable among the *APOE* genotypes. (A) Representative images of cortex in sagittal brain sections from 2 and 4 month EFAD mice immunostained for Aβ (red) and NeuN (green), 20x magnification (scale bar = 20μm). Total number of Aβ-containing neurons in the **(B)** frontal cortex at 2 and 4 months (**C)** subiculum at 2 and 4 months, and **(D)** CA3 at 4 and 6 months in EFAD mice counted via unbiased stereology. Data are expressed as mean ± SEM and were analysed by two-way ANOVA followed by Bonferroni multiple comparison post hoc analysis**.** $^{*}p < 0.05$ vs. 2 or 4 months.

Downloaded from www.jbc.org at University of Illinois at Chicago Library, on October 29, 2012

Figure 4. Total apoE levels are lower and total Aβ42 levels are higher in E4FAD mice compared with E2FAD and E3FAD mice. Total levels of **(A)** apoE and **(B)** Aβ42 in the cerebellum (CB), hippocampus (H), and cortex (CX) of 2, 4 and 6 month EFAD mice measured by ELISA (nm = not measured). Dashed line marks the mean of apoE within the CB < CX < H ($p < 0.001$). Data are expressed as mean ± SEM and were analysed by two-way ANOVA followed by Bonferroni multiple comparison post hoc analysis. $^{*}p < 0.05$ vs. 2 or 4 months, $^{\#}p < 0.05$ vs. apoE2 and apoE3, $^{\ddagger}p < 0.05$ vs. apoE3.

Figure 5. The lower levels of total apoE4 are the result of a decrease only in the TBSX extraction fraction. Extraction profiles of **(A)** apoE and **(B)** Aβ42 using a 3-step sequential protein extraction (TBS, TBSX and FA) in the hippocampus of 2, 4 and 6 month EFAD mice measured by ELISA. Data are expressed as mean ± SEM and were analysed by two-way ANOVA followed by Bonferroni multiple comparison post hoc analysis. $^{*}p < 0.05$ vs. 2 or 4 months, $^{\#}p < 0.05$ vs. apoE2 and apoE3.

Figure 6: Soluble Aβ42 and soluble oligomeric Aβ levels are higher in E4FAD mice compared with E2FAD and E3FAD mice. ApoE, Aβ42, and oAβ in the TBS/soluble extraction fraction of the **(A)** cortex and **(B)** hippocampus in 6-month EFAD mice measured by ELISA. Data are expressed as mean ± SEM and were analysed by one-way ANOVA followed by Tukey's multiple comparison post-hoc analysis. $^{\#}p < 0.05$ vs. apoE2 and apoE3.

Downloaded from www.jbc.org at University of Illinois at Chicago Library, on October 29, 2012

Figure 1

A. Aβ progression in 5xFAD and EFAD mice

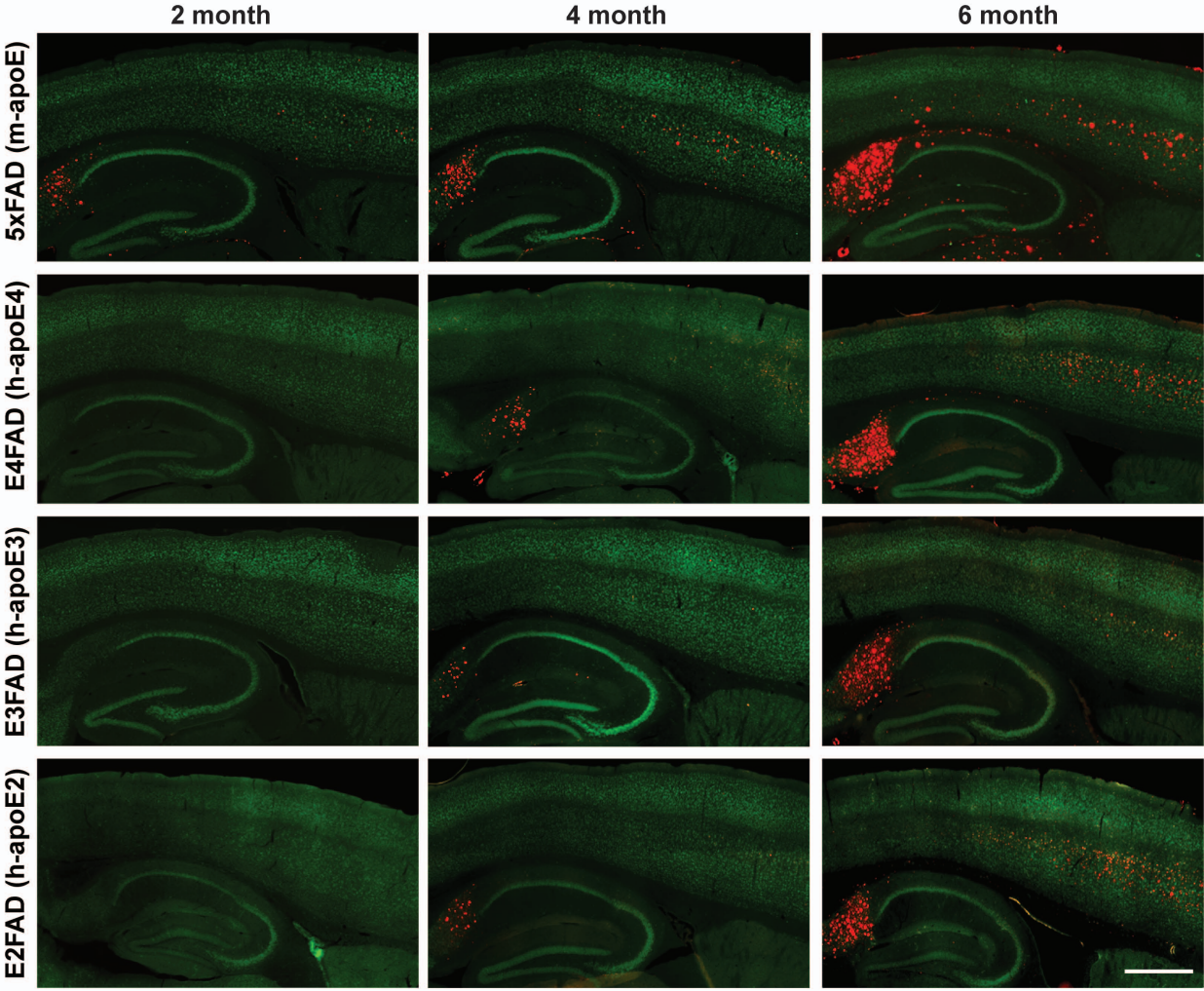

B. Total Aβ42 in hippocampus (6 months): 5xFAD vs EFAD

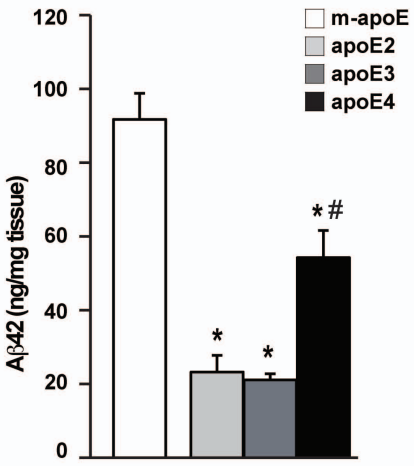

Figure 2

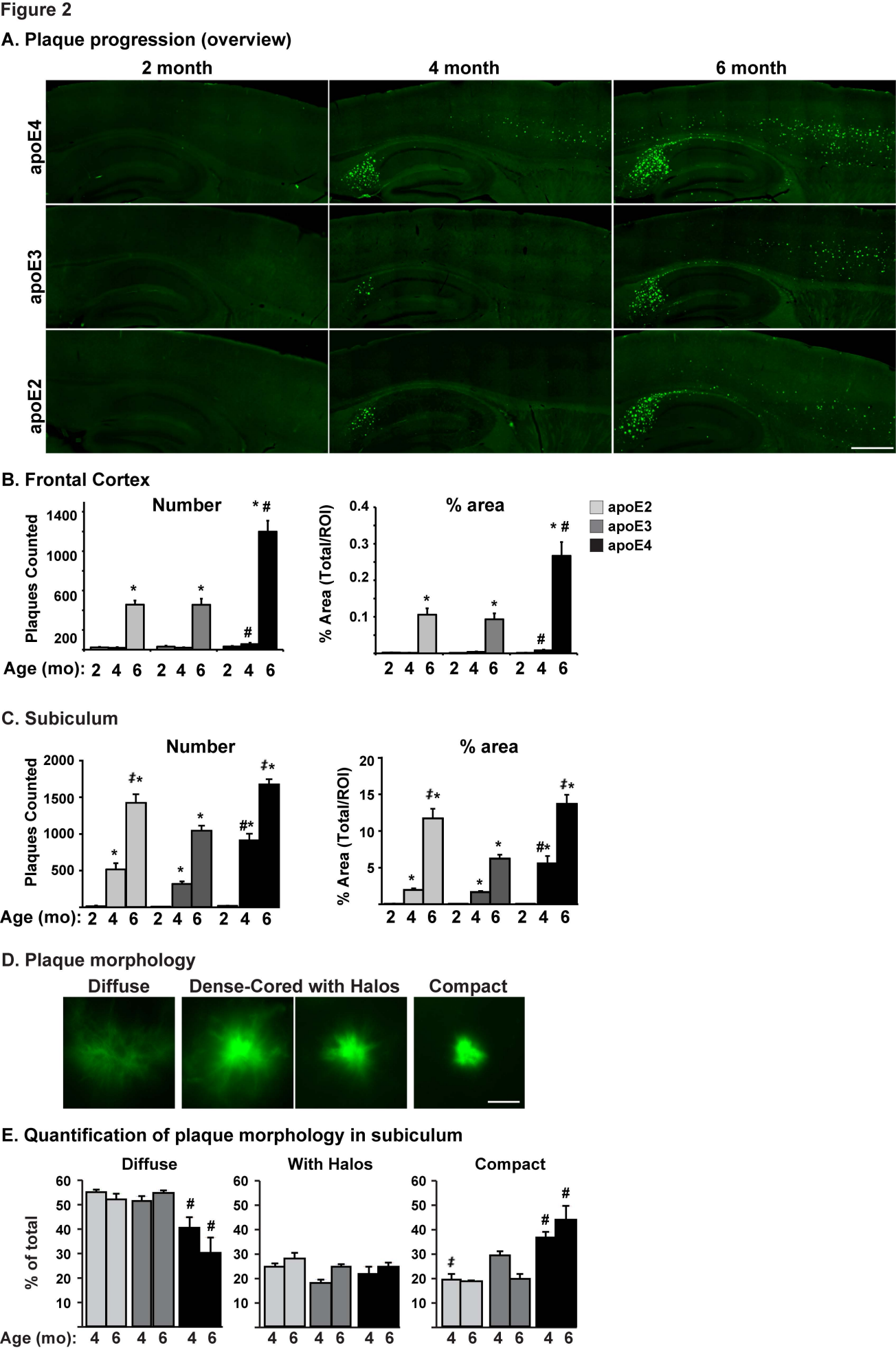
A. Plaque progression (overview)
2 month
4 month
6 month
apoE4
apoE3
apoE2
B. Frontal Cortex
Number
Plaques Counted
1400
1000
600
200
Age (mo): 2 4 6 2 4 6 2 4 6
% area
% Area (Total/ROI)
0.4
0.3
0.2
0.1
apoE2
apoE3
apoE4
C. Subiculum
Number
Plaques Counted
2000
1500
1000
500
% area
% Area (Total/ROI)
20
15
10
5
D. Plaque morphology
Diffuse
Dense-Cored with Halos
Compact
E. Quantification of plaque morphology in subiculum
Diffuse
With Halos
Compact
% of total
60
50
40
30
20
10
Age (mo): 4 6 4 6 4 6

Figure 3

A. Intraneuronal Aβ (frontal cortex)

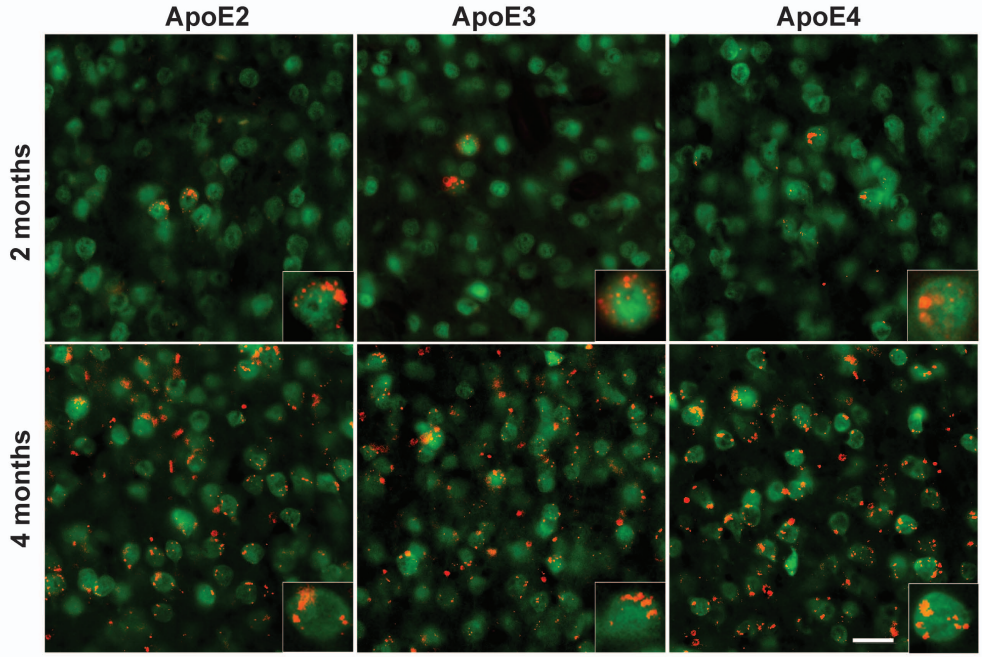

B. Frontal Cortex

C. Subiculum

D. CA3

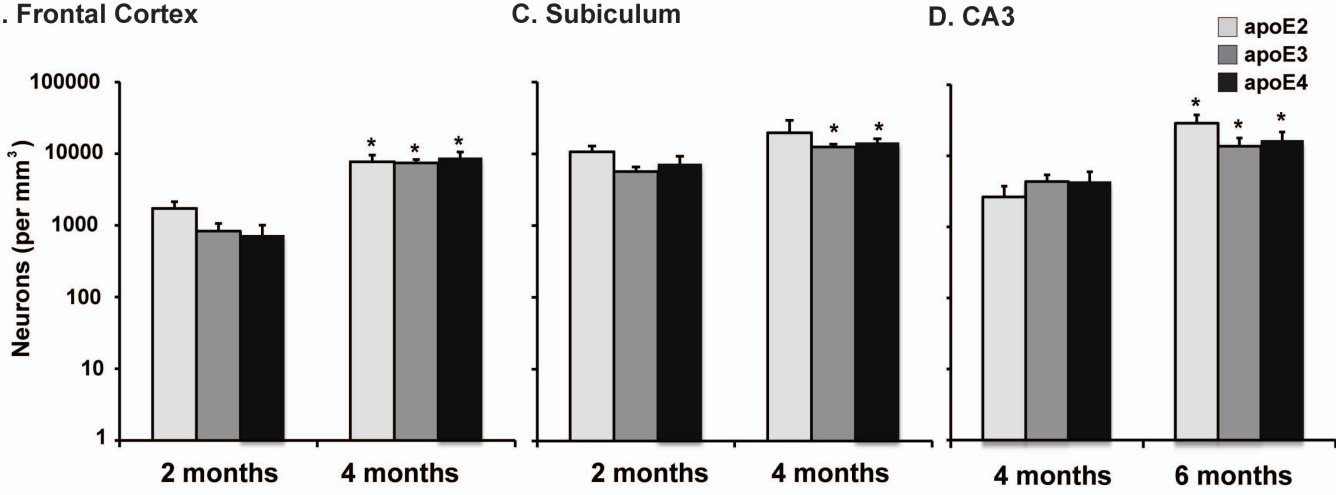

Figure 4

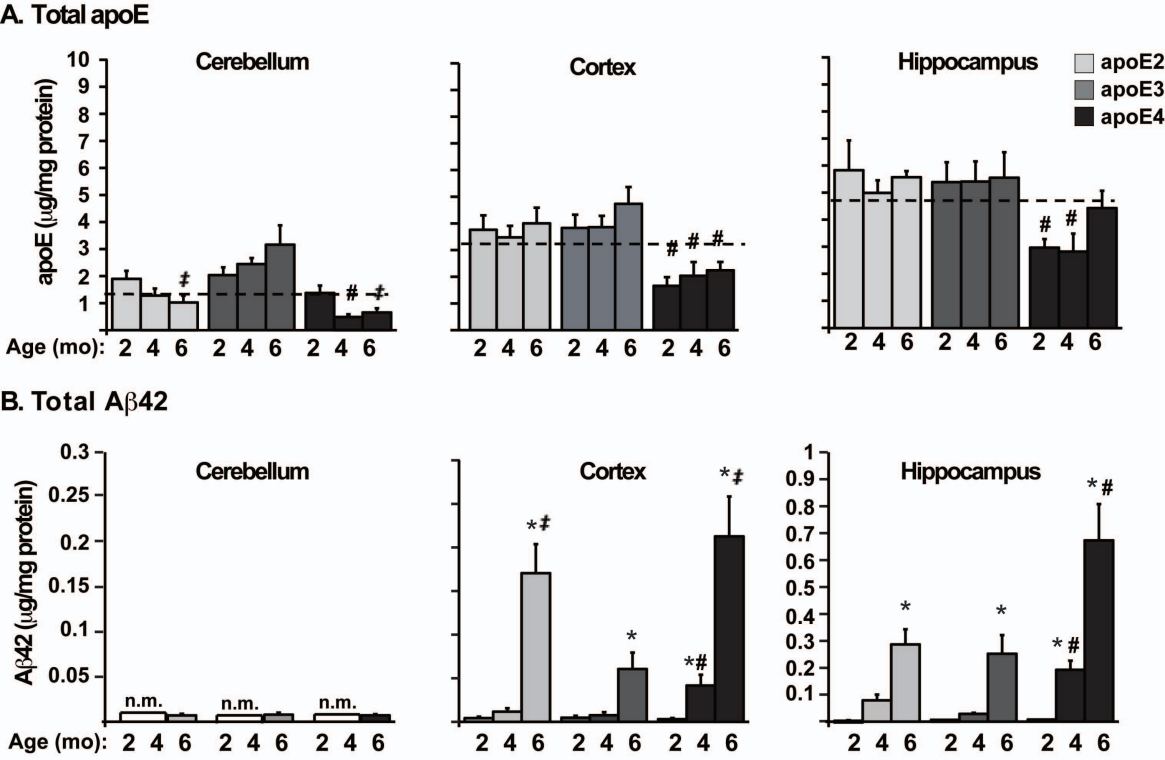
A. Total apoE
Cerebellum
Cortex
Hippocampus
apoE2
apoE3
apoE4
apoE (μg/mg protein)
Age (mo): 2 4 6 2 4 6 2 4 6
B. Total Aβ42
Aβ42 (μg/mg protein)
n.m.

Figure 5

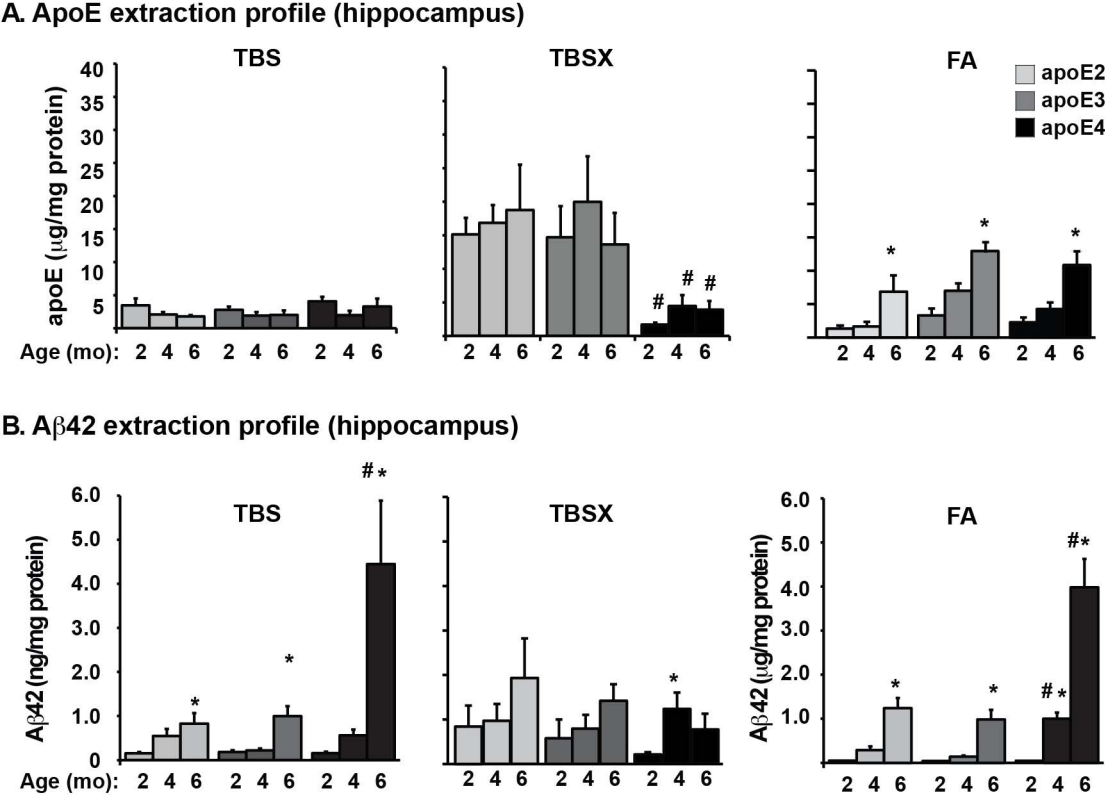
A. ApoE extraction profile (hippocampus)
TBS
TBSX
FA
apoE2
apoE3
apoE4
apoE (μg/mg protein)
40
35
30
25
20
15
10
5
Age (mo): 2 4 6 2 4 6 2 4 6
B. Aβ42 extraction profile (hippocampus)
Aβ42 (ng/mg protein)
Aβ42 (μg/mg protein)
6.0
5.0
4.0
3.0
2.0
1.0
0

Figure 6

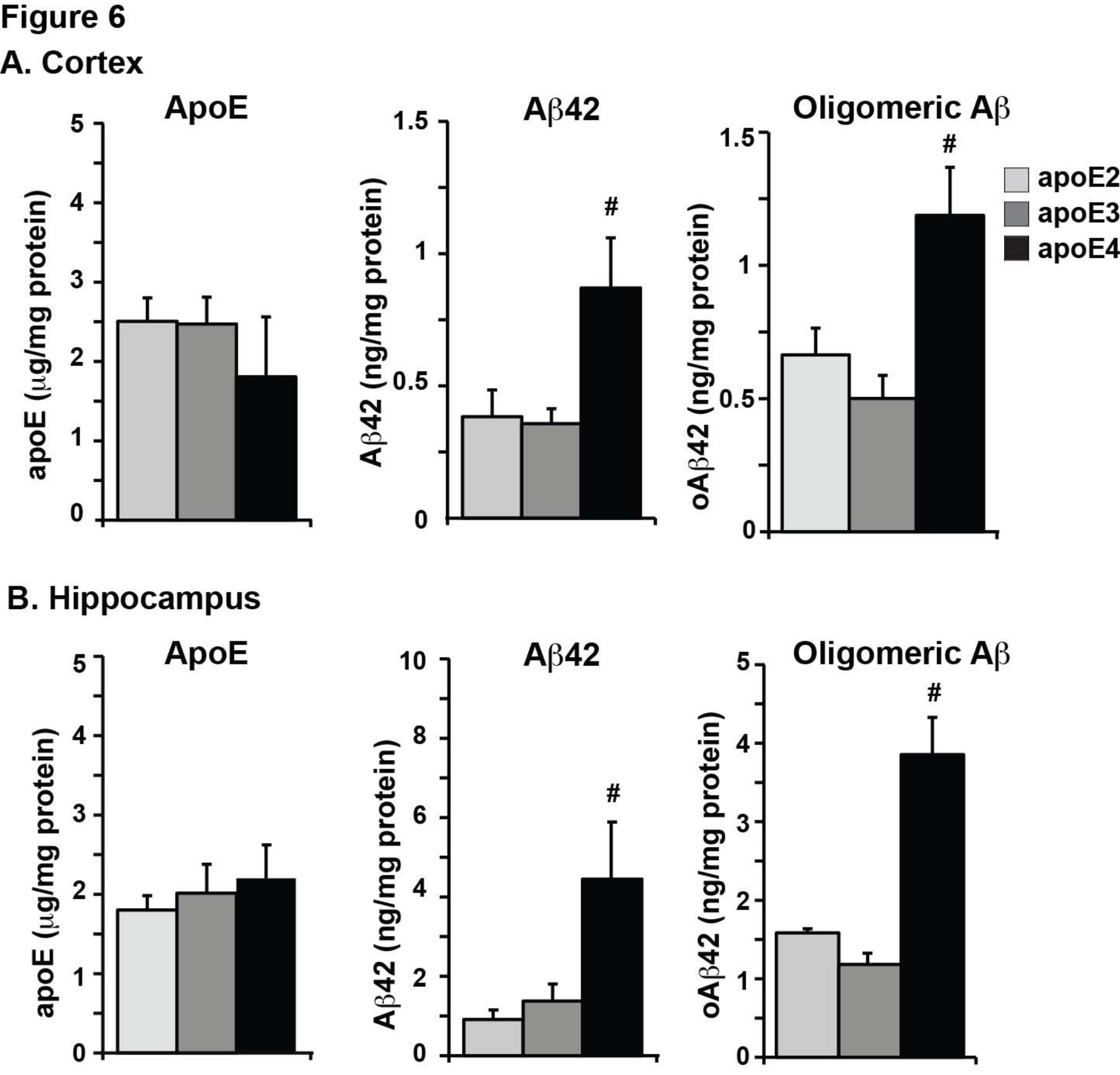
A. Cortex
ApoE
apoE (μg/mg protein)
0
1
2
3
4
5
Aβ42
Aβ42 (ng/mg protein)
0
0.5
1
1.5
#
Oligomeric Aβ
oAβ42 (ng/mg protein)
0
0.5
1
1.5
#
apoE2
apoE3
apoE4
B. Hippocampus
ApoE
apoE (μg/mg protein)
0
1
2
3
4
5
Aβ42
Aβ42 (ng/mg protein)
0
2
4
6
8
10
#
Oligomeric Aβ
oAβ42 (ng/mg protein)
0
1
2
3
4
5
#